International Journal of Power Electronics and Drive System (IJPEDS)
Vol. 6, No. 2, June 2015, pp. 337~347
ISSN: 2088-8694

An Improved Double Fuzzy PI Controller For Shunt Active Power Filter DC Bus Regulation

Nabil Elhaj*, Moulay Brahim Sedra*, Tarik Jarou*, Hind Djeghloud**
* Laboratory of High Energies, Engineering Sciences, and Reactors, Ibn Tofail University, Kenitra, Morocco
** Laboratory of Electrical Engineering, Constantine 1 University, Constantine, Algeria

Article Info

Article history:

Received Jan 30, 2015
Revised May 16, 2015
Accepted May 25, 2015

Keyword:

Harmonics
SAPF
SRF & PSF algorithms
DFPI DC voltage controller
Comparisons

ABSTRACT

This paper targets to demonstrate the importance of the choice of the algorithm references detection to be applied with a double fuzzy PI corrector (DFPI) for the control and the regulation of a shunt active power filter (SAPF) DC bus voltage. In a previous work, the synchronous reference frame (SRF) algorithm was applied and gave satisfactory results. In the present paper, the SRF is compared to the positive sequence of the fundamental of the source voltage algorithm (PSF) which offered better results regarding the power quality of the considered main utility feeding a variable DC RL load throughout a diode bridge. The results were carried out using computer simulation performed under MATLAB/Simulink environment. To make the obtained results more convenient, a comparison between the couples (SRF, PI), (PSF, PI), (SRF, DFPI), (PSF, DFPI) is added to prove the effectiveness of the couple (PSF, DFPI) in satisfying the compromise between a good regulation of the SAPF DC bus voltage and a good quality of filtering resulting in an improved quality of power.

Corresponding Author:

Nabil elhaj,
Laboratory of High Energies, Engineering Sciences and Reactors,
Ibn Tofail University,
Kenitra, Morocco.
Email: Nabilmaill@yahoo.fr

1. INTRODUCTION

Recently, improving the quality of energy in electrical distribution power utilities becomes a subject of great interest. The power quality of these utilities is mainly related to the voltage and current waveforms that should be sinusoidal and in phase each other. However, the power quality can be affected by the influence of many disturbances, these disturbances are found under different forms (harmonics, sags, unbalance, flickers and swells) [1]-[2].

To minimize the effect of disturbances on power quality several solutions are proposed as effective remediation namely active power filters (APFs) based on voltage source (VSIs) or current source (CSIs) inverters that can be connected in parallel, series or both of them between the power utility and the disturbing load [3]-[4]. The principle of these topologies is to provide the opposite disturbance that counters the existing disturbance, so that it can't attain the power utility.

To be effective in its operation the active power filtering system needs to be well supplied with a sufficient and non fluctuating DC voltage in its DC bus terminals and well controlled to provide the desired output signals. To achieve these conditions, the control circuit is designed on the basis of three main blocks: the algorithm that detects the reference signals, the corrector that compensates the fluctuations of the DC bus voltage and the modulator that generates the switching signals to be launched to the inverter switches gates. These three blocks work together to output the compensating signals. Thus, they must be carefully conceived

to avoid failing in operation of the APF system. Several kinds of theses blocks can be found in the literature [5]-[6], [7]-[8], [9]-[10].

In this paper two algorithms of reference currents detection are considered to be associated with the DFPI controller introduced in [11]. It's a matter of the synchronous referential frame (SRF) algorithm and the positive sequence of voltage source fundamental (PSF) algorithm. The objective is to conclude about the most suitable algorithm to be applied with the DFPI controller intended to regulate the DC bus voltage of a shunt APF system. The pulses generator is a hysteresis modulator and the validation of the presented studies is based on simulation works performed under MATLAB/Simulink.

This work is summarized in five sections. Section 2 concerns the description of the considered topology and control technique. Section 3 presents the algorithms SRF and PSF. Section 4 recalls the principle of the introduced DFPI [11]. Section 5 is consecrated to the verification by computer simulation and to the comparative studies.

2. DESCRIPTION OF THE CONSIDERED TOPOLOGY AND CONTROL TECHNIQUE

Figure 1 shows the studied system that consists of a three phase power supply and its internal impedance (R_sL_s), a nonlinear load (diode rectifier) and a shunt active power filter. The rectifier loaded by a passive circuit (R_LL_L). The SAPF comprises a three-phase voltage inverter and an output filter (R_f L_f). This inverter is formed by a three half-bridges (T_1-T_4, T_2-T_5, T_3-T_6) based on IGBTs with anti-parallel diodes. The inverter legs are fed by a DC voltage V_{dc}. To generate the IGBTs pulses a hysteresis current controller is used. The reference currents are achieved first by the SRF algorithm, then by the PSF algorithm. The regulation of the DC voltage of SAPF is based on a Double Fuzzy logic PI controller [11]-[12]. A resistor R_{dc} is added to the system which is connected in parallel to the capacitor C_{dc} feeding the SAPF through the regulating loop. The role of this resistor is to minimize V_{dc} ripples by controlling the constant time τ as explained in (1).

$$R_{dc} = {}^{\tau}/_{C_{dc}} \quad (1)$$

Where C_{dc} is dimensioned in [11] and τ takes as value few alternances of the fundamental frequency [13]. The other passive elements and V_{dc} are also dimensioned in [11].

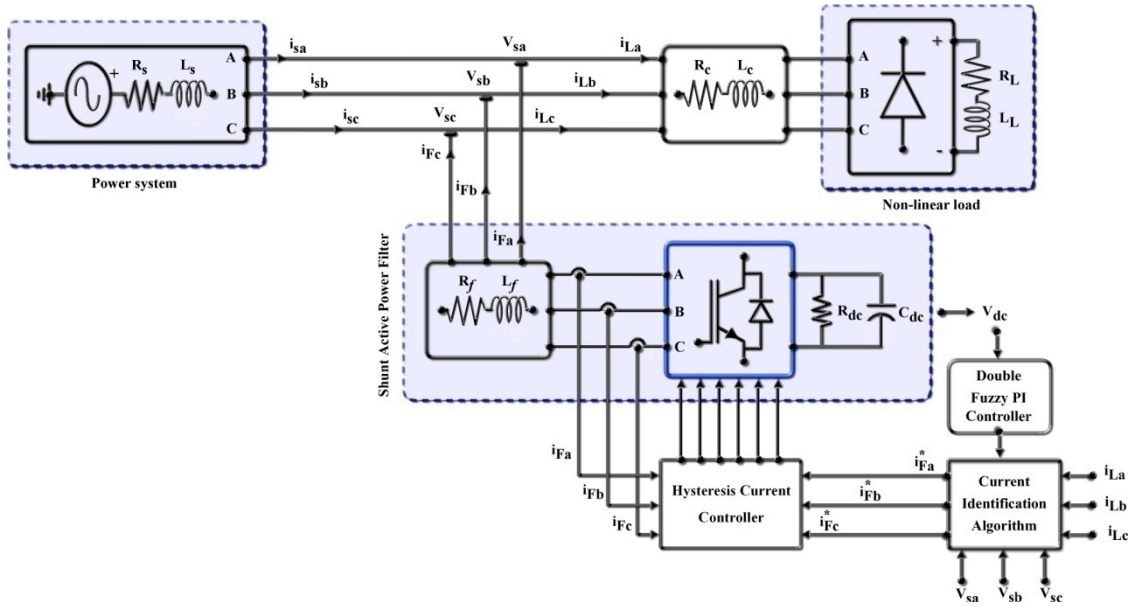

Figure 1. Schematic diagram of the studied system

3. SRF & PSF ALGORITHMS FOR REFERENCE DETECTION

a. SRF Algorithm

The principle of this algorithm is to force the source current to have the same angular frequency as that of the source voltage (i.e. source voltage and current waves are in synchronism each other), in this way

the power factor is forced to remain near the unity. The extraction of the reference currents is based on the Park transformation applied to the load three-phase currents so that the angle is procured from source three-phase voltages angular frequency through a three-phase PLL. Then from the obtained diphase load currents, fundamental part is removed using a 2nd order low-pass filter tuned on the fundamental frequency and which remains are the desired diphase reference currents as expressed in (2). Finally by using the inverse Park transformation, the three-phase reference currents are carried out. All these steps are summarized in the set of equations (2)-(4) and illustrated in the synoptic scheme of Figure 2 [14].

$$[i^*_{Fabc}] = [P]^{-1}.[i^*_{Fdq}] \quad (2)$$

Where $[P]^{-1}$ is the inverse of the Park transformation [P] [15], i^*_{Fdq} are the diphase reference currents given by (3).

$$[i^*_{Fdq}] = [i_{Ldq}] - [i_{Ldqdc}] \quad (3)$$

With:

$$[i_{Ldq}] = [P].[i_{Labc}] \quad (4)$$

And i_{Ldqdc} are outputs of the second order low-pass filter tuned on the fundamental frequency.

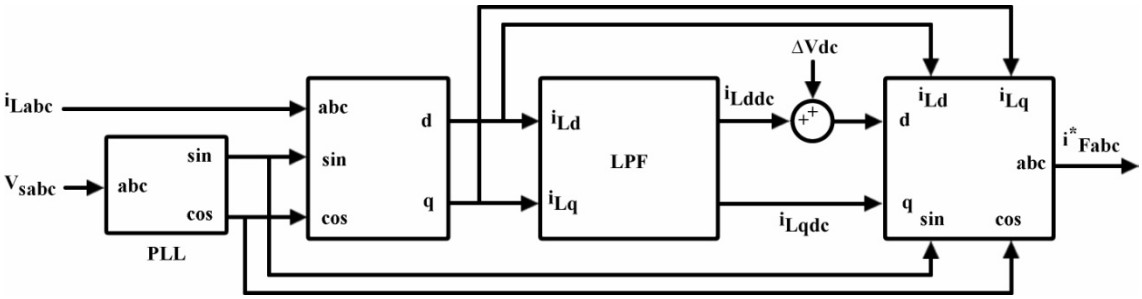

Figure 2. Synoptic scheme of the SRF algorithm (neglecting the zero sequence)

b. PSF Algorithm

The objective of this algorithm is also to keep the power factor around the unity but this time by forcing the source current to have the same argument as that of the positive sequence of the source voltage fundamental component. Thus the first step of the algorithm is to extract fundamental components from the source voltages using a second order band-pass filter. Then, the obtained instantaneous signals are converted into complex signals with help of Fourier block. Afterward, positive sequence of these complex signals is extorted through the Fortescue transformation. From this positive sequence component, the module will serve together with load active power to compute the module of the fundamental component of the source current as expressed in (5), whereas the argument will be the angle of this current. Then, from the total load current, the new current is removed; as a result a pure harmonic reference current is produced. The algorithm is illustrated in Figure 3 [16].

$$I^+_{sm} = \frac{2}{3}.\frac{P_L}{V^+_{smf}} \quad (5)$$

The demonstration of this equation is given in [16]. The reference currents are then expressed by (6):

$$\begin{bmatrix} i^*_{Fa} \\ i^*_{Fb} \\ i^*_{Fc} \end{bmatrix} = \begin{bmatrix} i_{La} \\ i_{Lb} \\ i_{Lc} \end{bmatrix} - I_{sm}.\begin{bmatrix} \sin(\omega t + \varphi^+_f) \\ \sin(\omega t - 2\pi/3 + \varphi^+_f) \\ \sin(\omega t + 2\pi/3 + \varphi^+_f) \end{bmatrix} \quad (6)$$

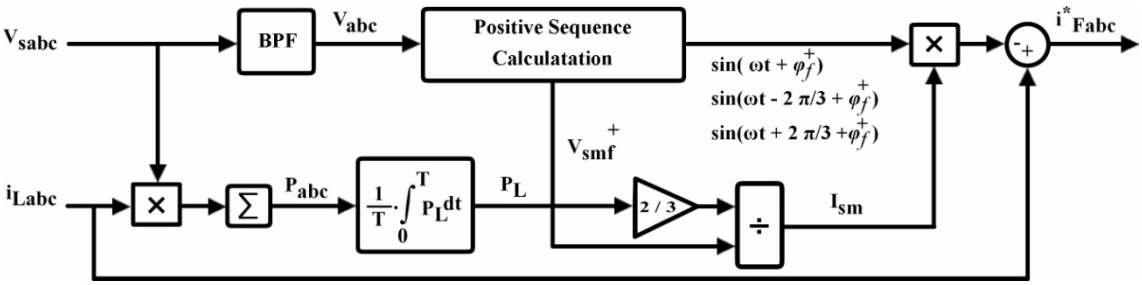

Figure 3. Synoptic scheme of the PSF algorithm

4. THE DFPI CONTROLLER

a. Principle of V_{dc} regulation

Fuzzy logic controller is used for complicated systems and allows translating knowledge and human reasoning to simple rules that a computer can use, while artificial intelligence and PI Control are used to achieve this objective. The diagram of Figure 4 shows the control algorithm of the capacitor voltage of the SAPF DC, this control is based on a double fuzzy PI controller. The DC bus voltage capacitor is compared with the reference to obtain the error 'e' given by the following equation:

$$e(t) = V_{dc}^{*}(t) - V_{dc}(t) \quad (7)$$

The reference voltage V_{dc}^{*} corresponds to the charge of the capacitor C_{dc}, these quantities are dimensioned in [11]. The derivative of the error is given by (8).

$$\Delta e(t) = e(t) - e(t-1) \quad (8)$$

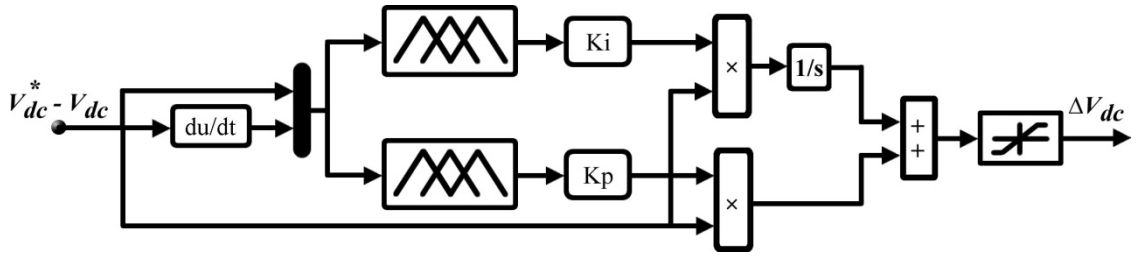

Figure 4. The proposed DFPI Controller for V_{dc} regulation

b. Structural construction of the fuzzy controller

The structural diagram of a fuzzy controller is shown in Fig.5. It consists of four distinct blocks [17]:

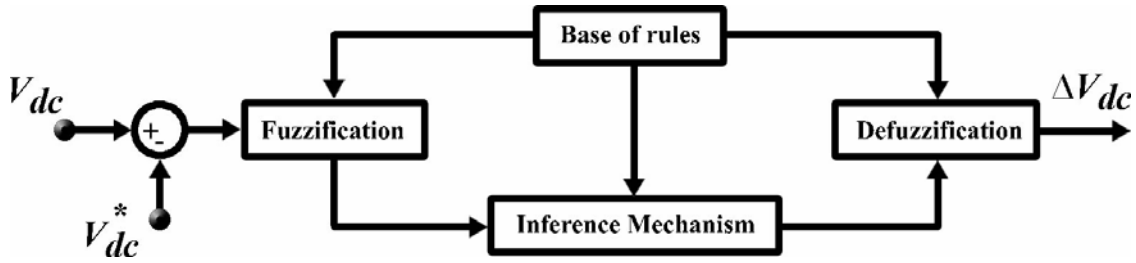

Figure 5. The structural diagram of the fuzzy controller

1. Base of rules

It consists on the establishment of the fuzzy rules based on the direction of variation of the error 'e', and the algebraic sign of the error 'e' and its derivative 'Δe'.

2. Fuzzification interface

In this step the membership functions of the input/output for each fuzzy partition of the universe of discourse are defined (Figure 6).

3. Inference mechanism

It is the process of designing fuzzy rules like: If e is ... & Δe is ... So ... the command is.

4. Defuzzification interface

In this step real value assigned to the variables of fuzzy output (several methods are available and most of them use the centroid or the bisector methods).

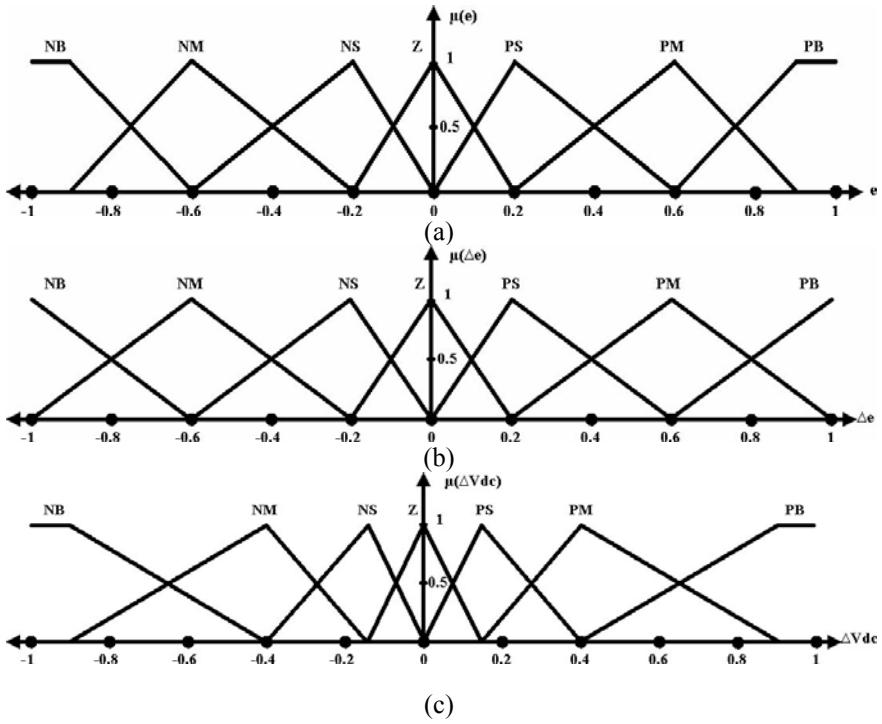

Figure 6. Membership function used in fuzzification for a) input variable e, b) input variable Δe, and c) output variable ΔV_{dc}

As shown in Figure 6 the fuzzification consists in using triangular membership functions for 'e' and its derivative 'Δe'. The inference mechanism describes 49 fuzzy rules summarized in Table 1, The linguistic values are defined as follows: {Positive Big (PB), Positive Medium (PM), Positive Small (PS), Zero (ZO), Negative Small (NS), Negative Medium (NM), Negative Big (NB)}. For defuzzification, the bisector method is applied.

Table 1. Fuzzy rules table

Δe/e	NB	NM	NS	Z	PS	PB
NB	NB	NB	NB	NB	NM	NS
NM	NB	NB	NB	NM	NS	Z
NS	NB	NB	NS	NS	Z	PS
Z	NB	NM	Z	Z	PS	PM
PS	NM	NS	PS	PS	PM	PB
PM	NS	Z	PM	PM	PB	PB

c. Dimensioning of the PI controller

The harmonic currents influence on the stability of the capacitor voltage and causes a corrugation of this latter. To reduce the ripples of DC voltage, a PI controller is used. The dimensioning of coefficients K_p and K_i of the PI can be achieved starting from the following diagram (Figure 8) which leads to the transfer function of the corrected system in the open loop expressed by (9).

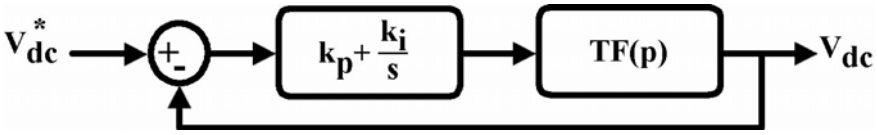

Figure 7. Coefficients Dimensioning of PI controller

$$TF_{without\ PI} = TF_i(p).TF_v(p) \tag{9}$$

Where,

$$TF_i(p) = \frac{i_F(p)}{V_F(p)} \quad \text{and} \quad TF_v(p) = \frac{V_{dc}}{i_F} \tag{10}$$

Where i_F and V_F are active components of the SAPF output current and voltage.

The passing band of the voltage loop is inferior to that of the current loop, consequently the pole of $TF_i(p)$ will not intervene in the voltage loop stability, so one can consider that $TF_i(p) = 1$ [18]. **By neglecting the switching losses in the active filter and in the output filter, the energy is the same in both DC and AC sides. Thus:**

$$dE_{dc} = C_{dc}.V_{dc}^*.\frac{d}{dt}V_{dc}.dt = P_{ac}.dt \tag{11}$$

Where,

$$P_{ac} = 3.V_{FRMS}.i_{FRMS} = \frac{3}{\sqrt{2}}.V_{FRMS}.i_{Fmax} \tag{12}$$

Therefore,

$$TF_v(p) = \frac{V_{dc}}{i_{Fmax}} = \frac{3.V_{FRMS}}{\sqrt{2}.C_{dc}.V_{dc}^*.p} = \frac{1}{a.p} \tag{13}$$

With,

$$a = \frac{\sqrt{2}.C_{dc}.V_{dc}^*}{3.V_{FRMS}} \tag{14}$$

Now by introducing the PI controller, the transfer function for the open loop becomes:

$$TF_{PI+v} = \left(K_p + \frac{K_i}{p}\right).\frac{1}{a.p} = \frac{1+\alpha_1.p}{\alpha_2.p^2} \tag{15}$$

Where,

$$\alpha_1 = \frac{K_p}{K_i} \quad \text{and} \quad \alpha_2 = \frac{a}{K_i} \tag{16}$$

In the periodical state, TF_{PI+v} is expressed as:

$$TF_{PI+v} = \frac{1+j\frac{\omega}{\omega_1}.p}{j^2(\frac{\omega}{\omega_0})^2} \tag{17}$$

So that,

$$\alpha_1 = \frac{1}{\omega_1} \quad \text{and} \quad \alpha_2 = \frac{1}{\omega_0^2} \tag{18}$$

According to Bode diagram of TF_{PI+v}, ω_0 and ω_1 can be deduced from the cutting frequency $\omega_c = 2.\pi.f_c$ for which the gain of $TF_{PI+v} = \left(\sqrt{1+(\frac{\omega_c}{\omega_1})^2}\Big/(\frac{\omega_c}{\omega_1})^2\right)$ is null and its phase φ equals $\text{atan}\,(\omega_c/\omega_1)$. Finally,

$$\omega_1 = \frac{\omega_c}{\tan(\theta)} \quad \text{and} \quad \omega_0 = \frac{\omega_c}{\sqrt{2}} \tag{19}$$

Generally, the cutting frequency is set at 20 Hz [18].

5. VERIFICATION BY COMPUTER SIMULATION

In this section simulation works about the previous study are provided. They were carried out using MATLAB/Simulink software and considering the parameters reported in Table 2.

Table 2. Simulation Parameters

Parameter	Value
AC supply voltage and frequency	380V-50Hz
Supply impedance	R_s = 0.07 Ω, L_s = 0.25 mH
Rectifier load	R_L = 10 Ω, L_L = 50 mH
Output filter impedance	R_F = 10 mΩ, L_F = 0.95 mH
Upstream filter impedance	R_c = 0.387 Ω, L_c = 0.3 mH
DC link capacitor	C_{dc} = 3.1 mF
DC Résistance	R_{dc} = 64.5 Ω
DC link reference voltage	V_{dc}^* = 550 V
PI angle, coefficients and saturation	60°, K_p = 0.1, K_i = 7.28, ±5V

The simulations models concern for pairs of (algorithm of references, V_{dc} controller) considering (SRF, PI), (SRF, DFPI), (PSF, PI) and (PSF, DFPI). The obtained results are presented in the figures 8 to 13, note that only results of phase *a* are presented since there is similarity with the other phases shifted by ±120° from *a*.

Figure 8 presents the source current before performing the filtering operation. A nonsinusoidal wave can be seen in Figure 8.a. The harmonic spectrum of this wave gives a THD% of 25.48% which is not conform to the standards IEEE 519 and IEC 61000-3-2. Besides, the current is not in phase with the source voltage which means that the PF is not close to the unity.

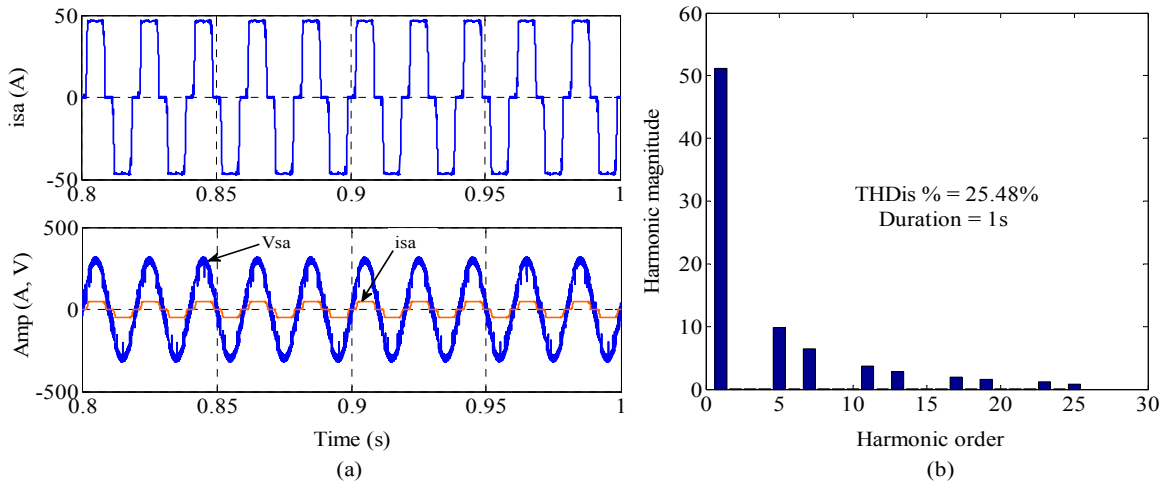

Figure 8. Results before starting the operation of the SAPF (a). Waveforms of V_{sa} and i_{sa} (b) Harmonic spectrum of i_{sa}

Figure 9 shows the results after putting the SAPF under operation but without inserting the controller of V_{dc}. The upper plot of Figure 9.a illustrates V_{dc} with its refrence V_{dc}^{*}, it is obvious that V_{dc} is inferior to V_{dc}^{*} (the deviation is around 6%). However the two other plots of Figure 9.b demonstrate a good quality of filtering in both current and source voltage as well as a good compensation of the power factor since no delay is noticed between the two signals. The THD% of the source current is 4.79% as depicted in Figure 9.c which agrees with the standards restrictions.

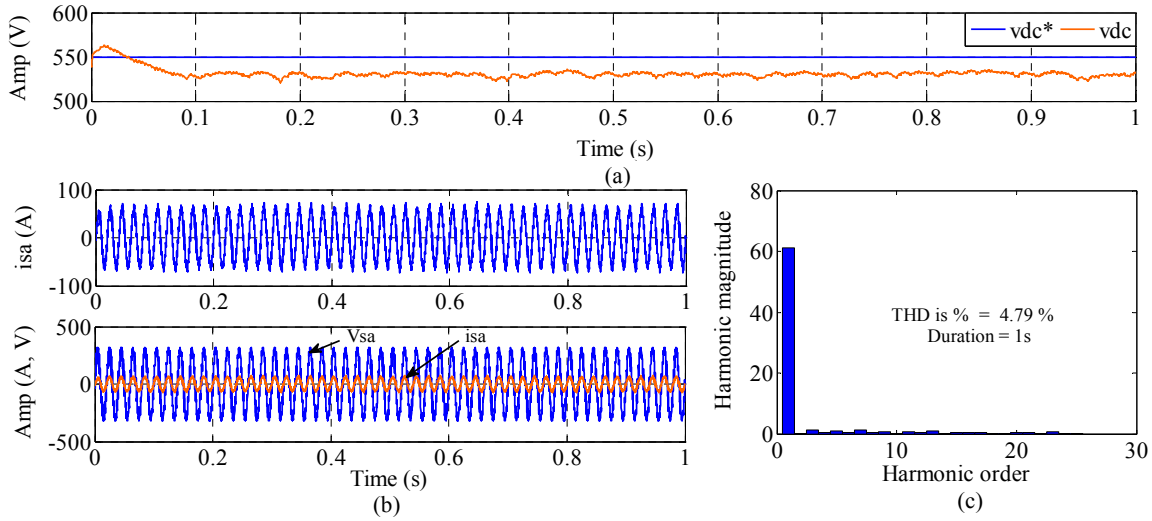

Figure 9. Results before inserting the V_{dc} controller (case of PSF algorithm).
(a) V_{dc} and V_{dc}^{*} (b) i_{sa} and i_{sa} with V_{sa} (c) Harmonic spectrum of i_{sa}

Figure 10 shows the obtained results after inserting the PI controller and using the SRF as algorithm for detecting the references of the SAPF currents. The first curve (Figure 10.a) mentions that V_{dc} follows perfectly its reference after a transient state of more than 0.3s. Concerning the filtering quality and the power factor compensation. Figure 10.b describes sinusoidal waveforms for both current and voltage in the source, moreover they are in phase which means a satisfactory value of the PF. Figure 10.c gives the THD% of i_{sa} which is also conform to norms (2.79%).

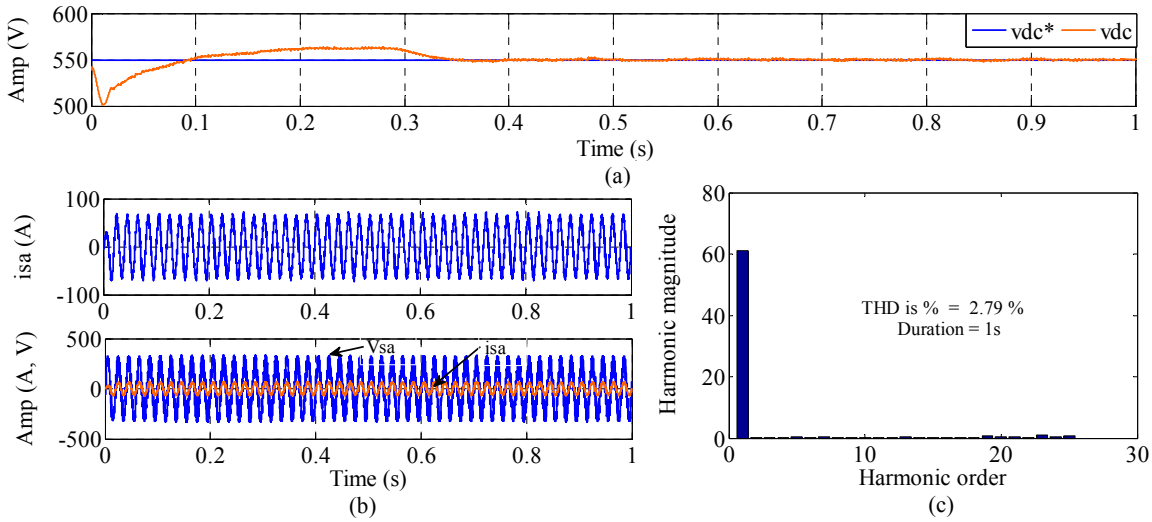

Figure 10. Results after inserting the PI controller associated to the SRF algorithm
(a) V_{dc} and V_{dc}^{*} (b) i_{sa} and i_{sa} with V_{sa} (c) Harmonic spectrum of i_{sa}

Figure 11 provides the results of the DFPI associated to the SRF algorithm. As shown in Figure 11.a, less transient state occurs (less than 0.1s), then V_{dc} reaches V_{dc}^{*} and evolves with it. The impact of the DFPI in reducing the transient state duration is very clear. Figure 11.b demonstrates the synchronism between source voltage and current whereas Figure 11.c indicates an acceptable THD% of i_{sa}. Which mean that the improvement introduced in V_{dc} regulation hasn't influenced the power factor and the filtering quality.

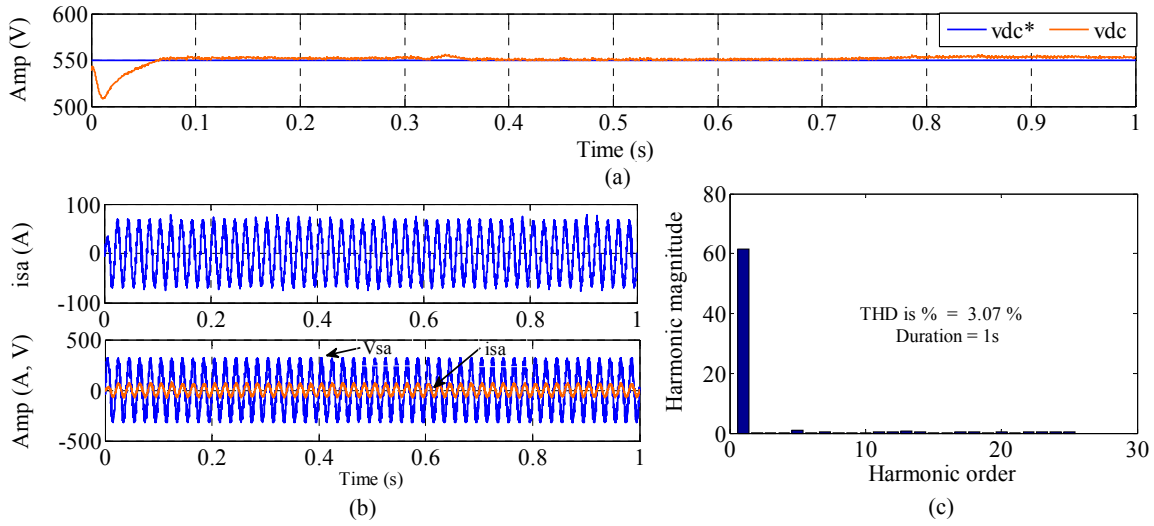

Figure 11. Results after inserting the DFPI controller associated to the SRF algorithm
(a) V_{dc} and V_{dc}^{*} (b) i_{sa} and i_{sa} with V_{sa} (c) Harmonic spectrum of i_{sa}

Now, results concerning the couples (PSF algorithm, PI controller), (PSF algorithm, DFPI controller) will be dressed. The objective is to carry out better results than those of the precedent couples (SRF algorithm, PI controller) and (SRF algorithm, DFPI controller). Fig.12 shows the results of the couple (PSF algorithm, PI controller). One can see better result in V_{dc} regulation comparing to that shown in Figure 11.a, the transient state in Figure 12.a describes an exceeding value of 25V, while Figure 11.a indicated a lack of 50V in the transient state. Although the obtained THD% of i_{sa} (3.89%) is greater than that of Figure 11.c (3.07%), but it remains conform to norms (< 5 %).

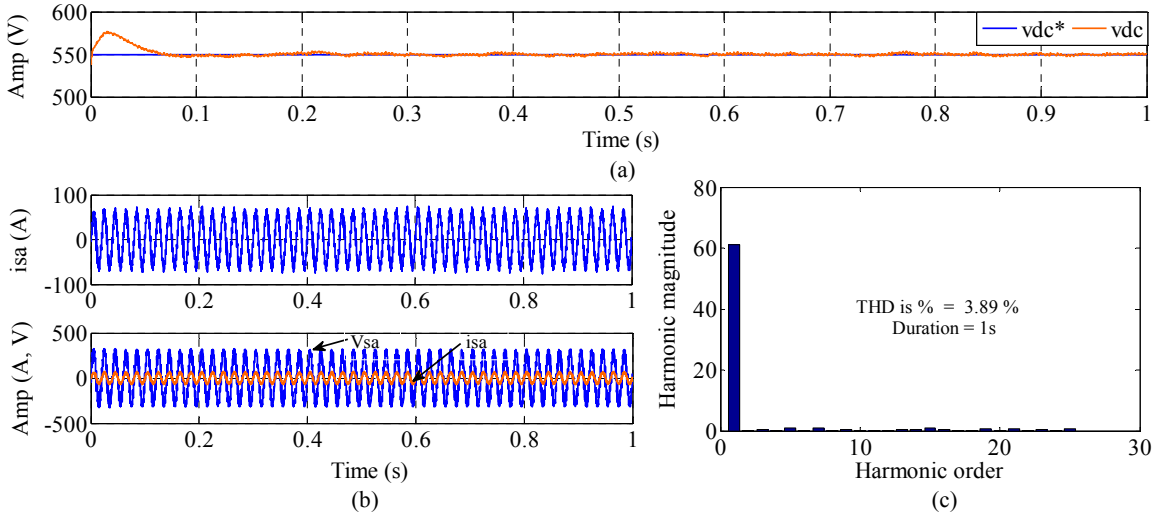

Figure 12. Results after inserting the PI controller associated to the PSF algorithm
(a) V_{dc} and V_{dc}^{*} (b) i_{sa} and i_{sa} with V_{sa} (c) Harmonic spectrum of i_{sa}

Finally Figure 13 gives the results of the last couple (PSF algorithm, DFPI controller).

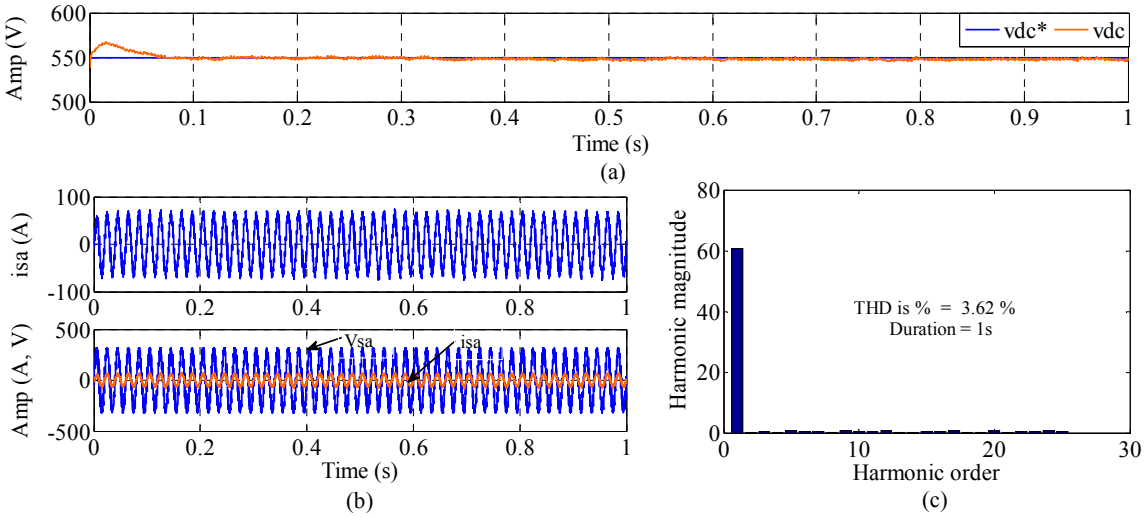

Figure 13. Results after inserting the DFPI controller associated to the PSF algorithm
(a) V_{dc} and V_{dc}^{*} (b) i_{sa} and i_{sa} with V_{sa} (c) Harmonic spectrum of i_{sa}

Obviously the regulation of V_{dc} is the best for this latest couple. In fact as depicted in Figure 13.a V_{dc} describes less exceeding value (< 25V) in the transient state comparing to Figure 12.a. Furtheremore the THD% of Figure 13.c (3.62%) is less than that of Figure 12.c. Consequently, one can conclude that the couple (PSF algorithm, DFPI controller) is the best in regulating V_{dc}, correcting the power factor and improving i_{sa} waveform.

6. CONCLUSION

In the objective of improving the results carried out in a former work, the present article has focused on changing the algorithm of detection of the reference currents of a SAPF to obtain better response simultaneously in regulating the DC voltage V_{dc} of the SAPF, maintaining the power factor at a satisfactory level and improving the filtering quality (obtaining a conform THD% of the source current). In the previous work, the SRF algorithm was used, it was associated to the DFPI V_{dc} controller. In this study, the SRF is compared to the PSF algorithm since it is based on the principle of forcing the fundamental source current to have the same angle as that of the positive sequence of the fundamental source voltage. Thus, the main feature of the PSF is to ensure a unity power factor in the source side. After presenting the considered algorithms and controllers, a verification through simulations were performed under MATLAB/Simulink environment which concerned four couples of algorithm/controller (SRF/PI, SRF/DFPI, PSF/PI, PSF/DFPI). The results indicated that the best couple satisfying the targets (less transient state and less exceeding value of V_{dc}, a unique PF and a conform THD% of i_s) is the couple (PSF/DFPI). The continuation of the study concerns the application of a DFPI controller for regulating the SAPF current.

REFERENCES

[1] A. Pavas, H. Torres, D. Urrutia, G. Cajamarca, L.E. Gallego and L. Buitrago, "A Novel Approach to the Simulation of Power Quality Disturbances in Electric Power Systems," IEEE/PES Transmission & Distribution Conference and Exposition: Latin America, 2006. TDC '06, Caracas, 15-18 Aug. 2006.
[2] Roger C. Dugan, Mark F. McGranaghan Surya Santoso, H. Wayne Beaty," Electrical Power Systems Quality, Second Edition," McGraw-Hill, 2004.
[3] H. Akagi, "The State-of-the-Art of Active Filters for Power Conditioning," in Rec. European Conference on Power Electronics and Applications, Dresden, pp. 1–15, September 2005.
[4] L. Morán & J. Dixon, "Active filters, Power Electronics Handbook," Academic Press, Chapter 39, pp. 1–36, 2007.
[5] D. Chen & S. Xie, "Review of the Control Strategies Applied to Active Power Filters," in Rec. IEEE International Conference on Electric Utility Deregulation, Restructuring and Power Technologies (DRPT2004), Hong Kong, April 2004.

[6] S. Zhang, D. Li & X. Wang, "Control Techniques for Active Power Filters," in Rec. International Conference on Electrical and Control Engineering, pp. 3493 – 3498, Wuhan 2010.
[7] G. A. Vargas Cáceres, J. C. GélvezLizarazo, M. A. Mantilla Villalobos & J. F. Petit Suárez," Active Power Filters: a Comparative Analysis of Current Control Techniques," in Rec. IEEE ANDESCON, Bogota, 2010.
[8] T. Demirdelen, M. Inci, K. C. Bayindir & M. Tumay, "Review of Hybrid Active Power Filter Tologies and Controllers," in Rec. 4th International Conference on Power Engineering, Energy and Electrical Drives, pp. 587-592, Istanbul 2013.
[9] Somlal Jarupula, Narsimha Rao Vutlapalli, "Power Quality Improvement in Distribution System using ANN Based Shunt Active Power Filter, " IJPEDS International Journal of Power Electronics and Drive Systems, Vol 5, No 4, 2015.
[10] Mridul Jha, S.P. Dubey , "Neuro-Fuzzy based Controller for a Three- Phase Four-Wire Shunt Active Power Filter," IJPEDS International Journal of Power Electronics and Drive Systems, Vol 1, No 2, 2011.
[11] N. Elhaj, T. Jarou, M. B. Sedra, H. Djeghloud & Y. Terriche, "Contribution of a Shunt Active Power Filter Control using Double Fuzzy PI Controller," in Rec.16th International Power Electronics and Motion Control Conference and Exposition, pp. 1177-1182, Antalya 2014.
[12] D. Wang et al., "Hybrid Active Power Filter DC Bus Control Based on Double Fuzzy Control," in Proc. of the 2nd Int. Conf. on Computational Intelligence and Natural Computing Proceedings (CINC), pp.287-290, Wuhan., 2010.
[13] M. Vial, "Electricité professionelle," Ed. Nathan, France, 1998.
[14] S. Bhatacharya & D. Divan, "Synchronous frame based controller implementation for a hybrid series active filter system," in Conf. Rec. IEEE-IAS Annu. Meeting, pp. 2531–2540, 1995.
[15] R.H, "Park Two Reaction Theory of Synchronous Machines," AIEE Transactions 48:716-730, 1929.
[16] G.W. Chang & T.-C. Shee, "A novel reference compensating current strategy for shunt active power filter control," IEEE Trans. Power Delivery, vol. 19, No. 4, pp. 1751-1758, 2004.
[17] P. Karuppanan and K.K. Mahapatra, "PLL with fuzzy logic controller based shunt Active Power Filter for harmonic and reactive power compensation", in Conf. Rec. Indian Int. Conf. on Power Electronics IICPE2010, pp. 1–6, 2010.
[18] P. Ladoux & G. Ollé, "Compensator of harmonics and reactive power," Compensateur d'harmoniques et de puissance réactive, Publication RESELEC 2002.